Supplementary Material - Have we measured how clouds respond to aerosols or how cloud retrievals respond to aerosols?

Antti Arola[1,*], Timo H. Virtanen[1], Antti Lipponen[1], Pekka Kolmonen[1], Tom Goren[2], Goutam Choudhury[2], Edward Gryspeerdt[3], Vishnu Nair[3], David Painemal[4], Hannes Keernik[5], Velle Toll[5], and Harri Kokkola[1,6]

[1]Finnish Meteorological Institute, Finland.
[2]Department of Environment, Planning and Sustainability, Bar-Ilan University, Ramat Gan, Israel
[3]Department of Physics, Imperial College London, UK
[4]NASA Langley Research Center, Hampton, VA, USA
[5]Centre for Climate Research, Institute of Physics, University of Tartu, Tartu, Estonia
[6]Department of Technical Physics, University of Eastern Finland, Kuopio, Finland
[*]Corresponding author: Antti Arola, antti.arola@fmi.fi

Null experiments for the ship tracks

To assess the potential impact of linear-interpolation–related errors on the logarithmic CF response in ship tracks (Fig 3), we additionally estimated the response using null experiments that are expected to yield no detectable signal in the absence of tracks.[1] In these experiments, the logarithmic CF response was computed after artificially displacing the hand-logged ship tracks by 50 or 100 km to the left or right, or by rotating the tracks by 45° clockwise around their centroids. The CF response derived from the true ship tracks differs markedly from that in the null experiments, both in magnitude and in temporal evolution. For the true ship tracks, the 5th–95th percentile ranges of logarithmic changes are 0.14 to 0.31 for CF_{SR} and 0.002 to 0.057 for $\mathrm{CF}_{\mathrm{cloudmask}}$. In contrast, the CF response in all null experiments remains within -0.05 to 0.06 and -0.016 to 0.017, respectively, and exhibits no systematic temporal variability. We also recomputed the logarithmic CF response using only the unpolluted reference polygons from one side of the track (either the right or left side). The resulting 5th–95th percentile ranges and temporal evolution for CF_{SR} and $\mathrm{CF}_{\mathrm{cloudmask}}$

are very similar to those obtained when averaging both unpolluted reference polygons, with ranges of 0.14 to 0.42 and 0.003 to 0.064, respectively. Overall, the tests demonstrate that for the tracks analysed, linear-interpolation–related errors are negligible relative to the observed CF response.

Visualization of sources of bias and error affecting cloud susceptibilities

Supplementary Figure S1 illustrates various sources of aerosol-dependent biases in cloud retrieval outcomes. It is important to note that 1) the magnification in Figure 1c) shows that small cumulus clouds are preferentially retrieved inside the plume, while similar thin clouds outside the plume are missed. 2) Figure 1d) shows that, outside the plume, parts of large clouds are more often excluded when retrieved cloud effective radius exceeds the limits of the MODIS radiative-transfer look-up tables (LUTs) - precomputed relationships between cloud properties and observed reflectance - beyond which retrievals fail. In both cases, if CF is based on successful retrievals, elevated aerosol level produces higher CF values. Comparing Figures 1a) and b), we see that when PCL clouds are neglected, small optically thin cumulus clouds - characterized by low liquid water path - are preferentially missed outside the plume, leading to a bias in the retrieved LWP. Including also the thinner small clouds makes the clouds outside and inside the plume more comparable, and reduces the average LWP. 3) Figure e) illustrates another source of bias: in the densest part of the Kilauea plume, the MODIS cloud mask erroneously assigns part of the aerosol plume as a water-phase cloud. Although most of these do not then have successful cloud retrievals, they still inflate cloud fraction estimates when CF is defined from the number of water-phase pixels. This highlights that even the seemingly robust CF definitions remain prone to aerosol-dependent biases, underscoring the overall difficulty of extracting unbiased cloud responses to changes in aerosol.

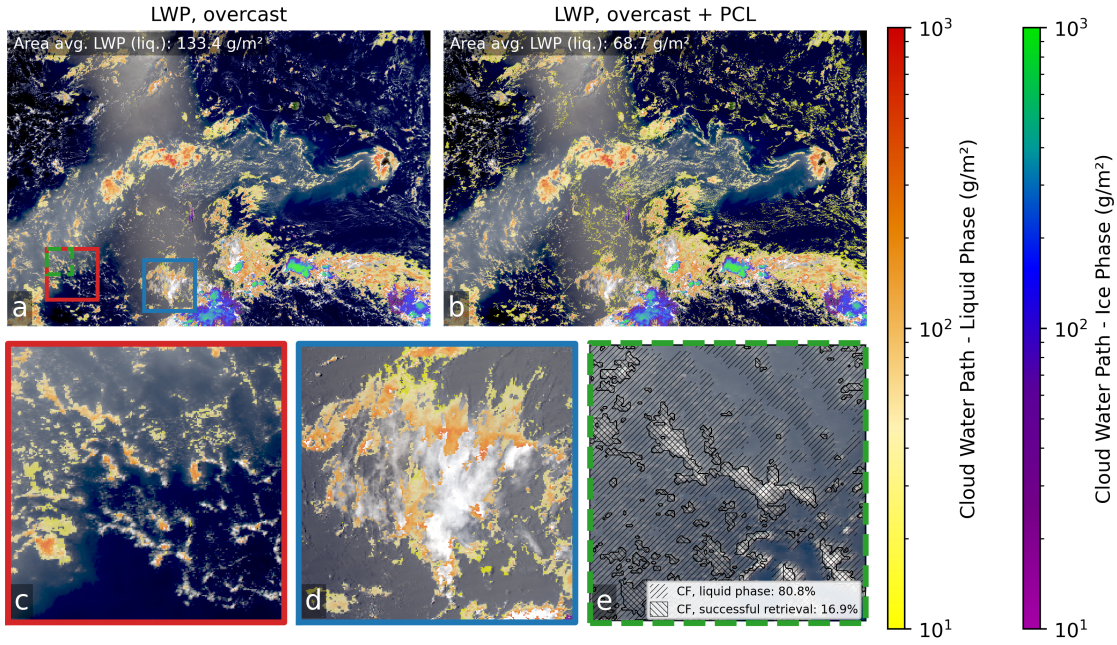

Supplementary Figure 1: Image from NASA's WorldView to illustrate the various sources of bias and error. The selected region is west of Kilauea volcanic eruption. a) LWP of overcast pixels, b) LWP of overcast pixels and of PCL (partly cloudy) pixels. c–e) Spatial subsets corresponding to the red, blue, and green boxes highlighted in a): c)-d) LWP of overcast pixels, e) forward-leaning hatching indicates water phase pixels. Successful retrievals within these regions are further highlighted with backward-leaning hatching.

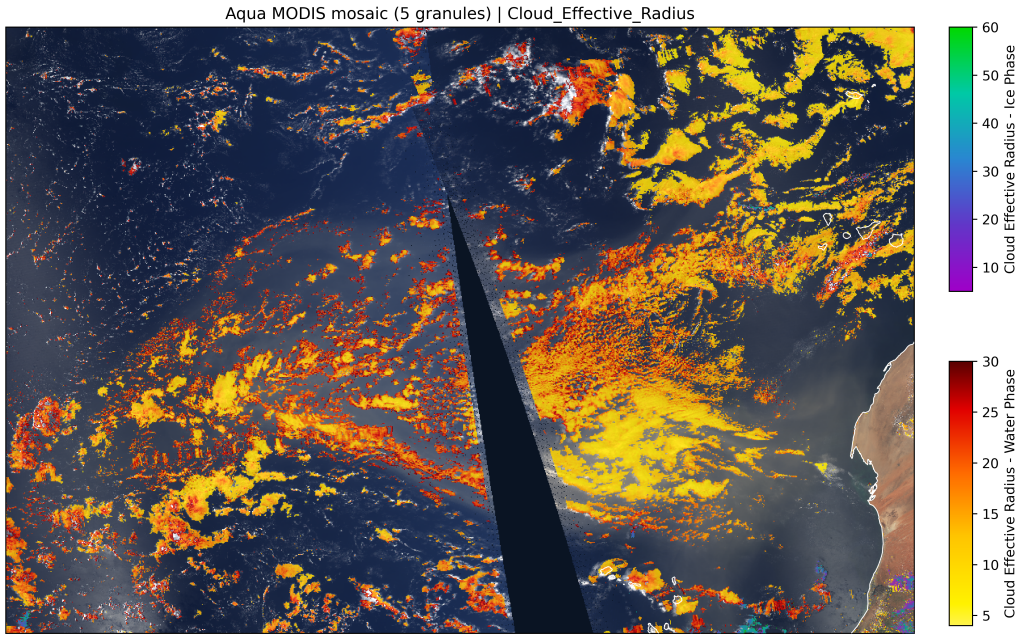

Supplementary Figure 2: Aerosol-dependent retrieval outcomes in a Saharan dust case. Imagery west of the Sahara on [27 August 2019, Aqua granules] illustrates that cloud-property retrievals succeed more frequently inside the dust plume than in adjacent background scenes.

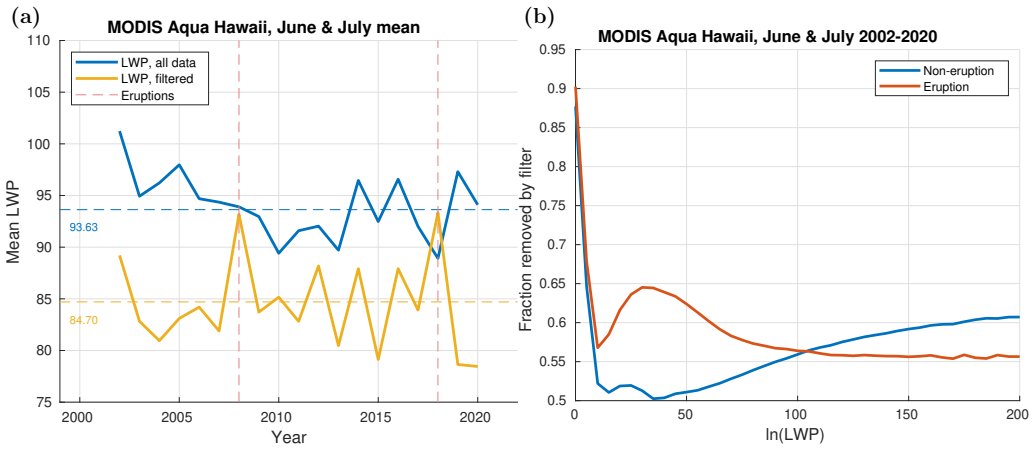

Supplementary Figure 3: a) Time-series of MODIS cloud liquid water path (LWP) averaged over the study area for June and July each year. The blue line shows the average values from all successfully retrieved cloud pixels, while for the yellow line the neighbor-consistency filter has been applied. The dashed horizontal lines show the total mean values for each line. The dashed vertical lines indicate the eruption years 2008 and 2018. b) Fraction of data removed by the neighbor-consistency filter per LWP bin for non-eruption years (blue line) and for eruption years (red line)

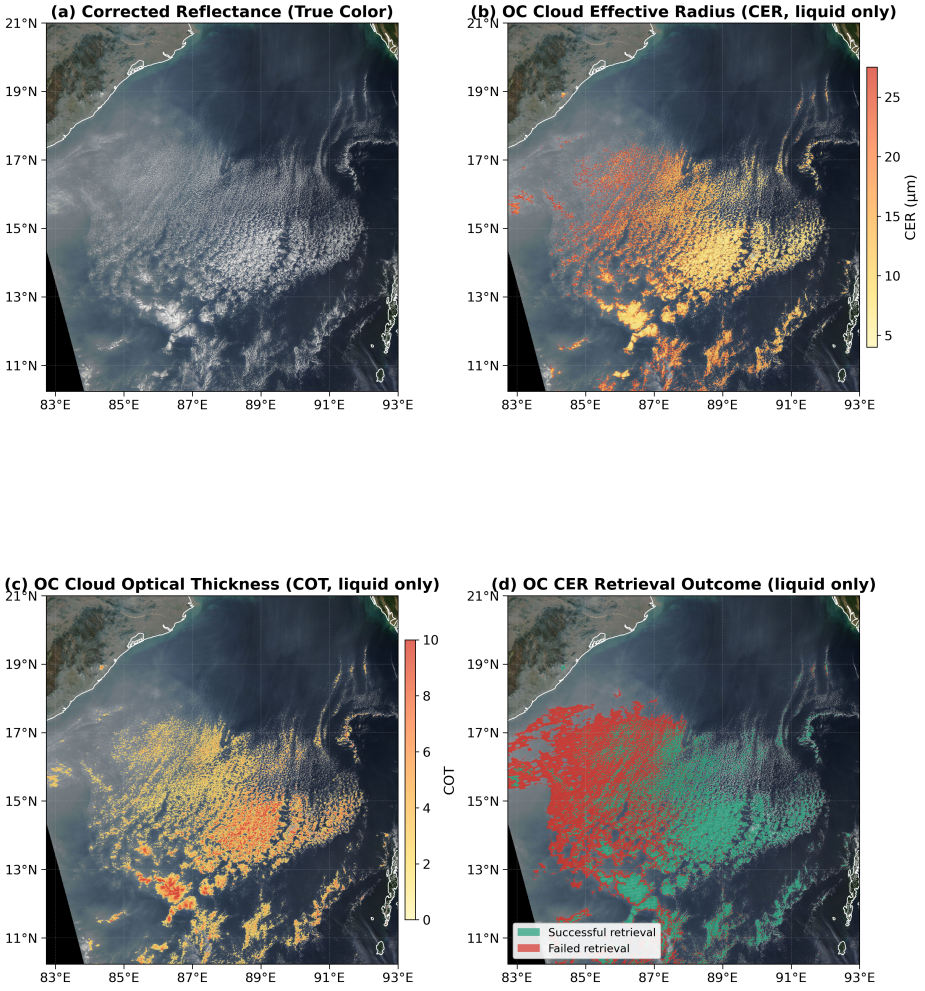

Supplementary Figure 4: Bay of Bengal case illustrating aerosol-dependent retrieval sampling. Aqua MODIS scene east of India (15 January 2017 granule). (a) True-color image showing an aerosol reflectance gradient toward the coast. (b) Overcast (OC) retrieval of cloud droplet effective radius (CER) and (c) cloud optical thickness (COT). (d) Retrieval outcomes: successful OC retrievals versus unsuccessful cases, defined as pixels identified as liquid-phase cloud for which the OC optical-property retrieval does not return CER/COT (e.g., observations outside LUT bounds).

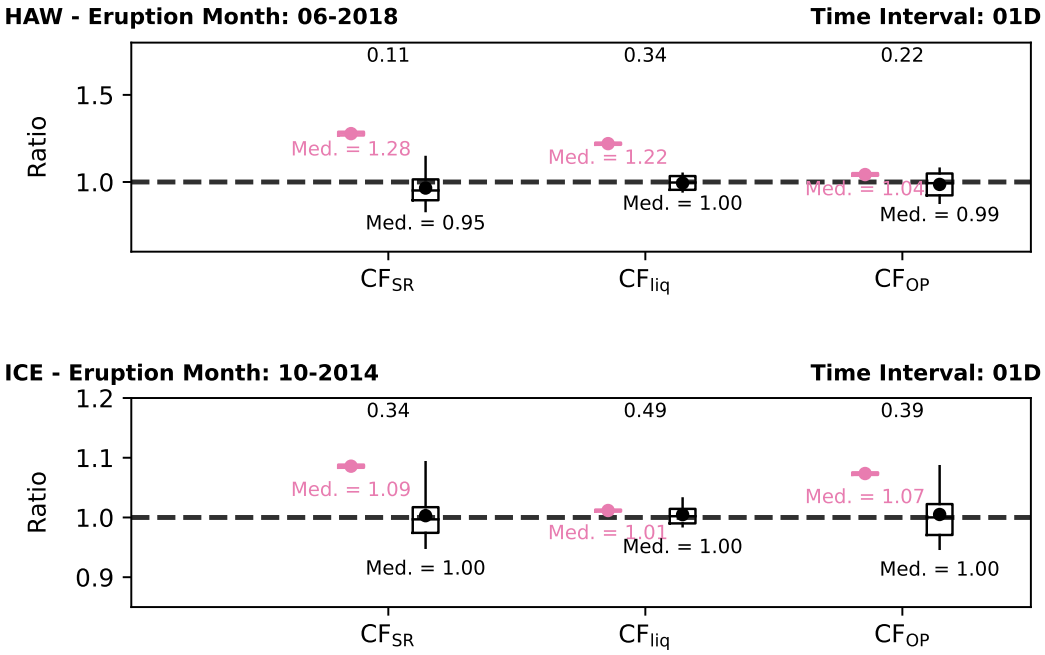

Supplementary Figure 5: Responses of cloud fraction (CF) to the Kilauea volcanic aerosol perturbation in June 2018 (upper panel) and to the Holuhraun in October 2014 (lower panel). Box-plots show the ratio of MODIS/MODIS_ML for the eruption year (pink) and non-eruption years (black). Different definitions for CF were used, from left to right in x-axis. Based on number of successful retrievals (in the left-hand side), based on the number of liquid phase pixels (in the middle), and based on successful retrievals from overcast and PCL (partly cloudy) retrievals (in the right-hand side). Daily data are used for clouds and meteorology.

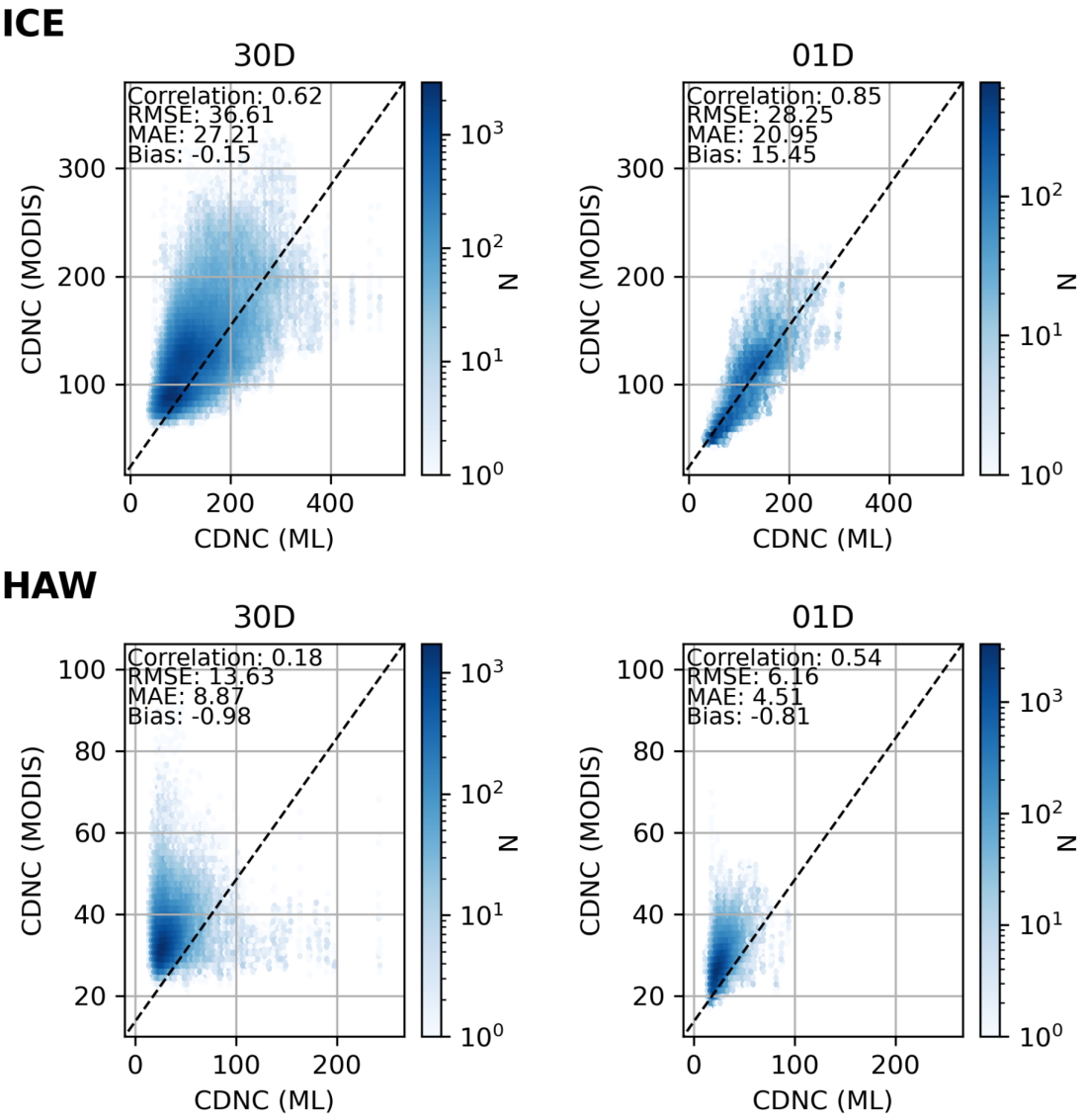

Supplementary Figure 6: Random Forest performance for non-eruption years for Holuhraun and Kilauea case. Cloud droplet number concentration with monthly (left-hand-side) vs. daily meteorology (right-hand-side).

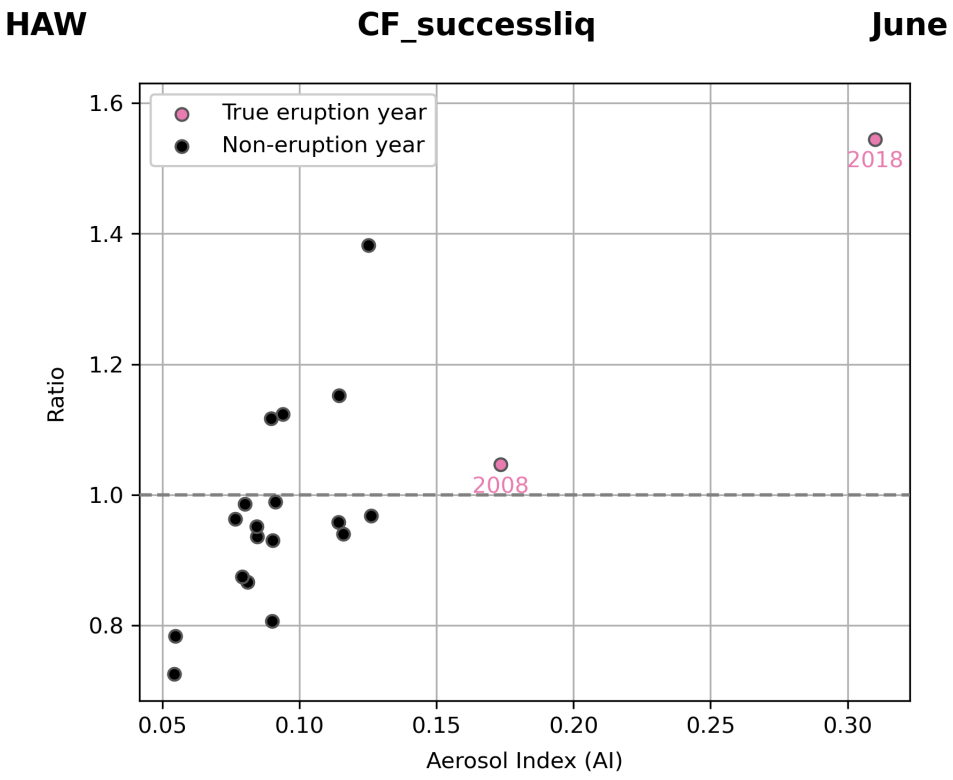

Supplementary Figure 7: Cloud fraction ratios (MODIS/MODIS_ML) as a function of aerosol index (AI), derived by repeating the pseudo-eruption analysis year by year. Both eruption years (2008 and 2018) do not stand out from the background variability, indicating that natural fluctuations can yield CF changes comparable to those attributed to aerosol effects, highlighting the limits of attribution in this framework.

Supplementary References

[1] Tippett, A., Gryspeerdt, E., Manshausen, P., Stier, P., and Smith, T. W. P.: Weak liquid water path response in ship tracks, *Atmospheric Chemistry and Physics*, **24**(23), 13269–13283, 2024. doi:10.5194/acp-24-13269-2024.